Ordering effects in thin smectic-C^* films: An x-ray-reflectivity study

E. Olbrich, O. Marinov, and D. Davidov
Racah Institute of Physics, The Hebrew University of Jerusalem, Jerusalem 91904, Israel
(Received 16 February 1993)

The x-ray-reflectivity technique is used to study the smectic order and the smectic-A (Sm-A) to smectic-C^* (Sm-C^*) phase transition in thin and ultrathin films (150–600 Å) of the chiral ferroelectric liquid-crystal mixture ZLI-3654 (produced by Merck). The films, which are spin cast on various substrates [very smooth (float) glass, Si wafer, polymer-coated glass, etc.], order spontaneously with smectic layering parallel to the substrate surface; the film alignment is induced by anchoring forces at the film-air interface. The reflectivity profiles could be well described by a sinusoidal density modulation perpendicular to the film. We demonstrate that it is possible to extract the molecular tilt angle α in ferroelectric liquid crystals from x-ray-reflectivity measurements of thin films. The Sm-A–Sm-C^* phase-transition temperature and the temperature dependence of the tilt angle in the smectic-C^* phase are almost independent of the film thickness (down to $\sim$200 Å) and are similar to those in the bulk. In all cases the dependence of the tilt angle $\alpha(T)$ can be described by a power law: $\alpha \sim t^{\gamma}$ ($t=1-T/T_c$), where $\gamma=0.31\pm0.04$, in agreement with the de Gennes predicted superfluid helium analogy [Acad. Sci. Paris Ser. B **274**, 785 (1972)]. In a film of about 200-Å thickness we observed a smectic layer spacing which is much larger than in thick films.

PACS number(s): 61.30.Eb, 61.10.−i, 68.55.−a

I. INTRODUCTION

There is a great deal of interest in the orientational and the structural wetting properties of liquid crystals (LC) at interfaces [1–9]. It is well known that surfaces can align liquid-crystal molecules through the anisotropic interaction between the molecules and the surface [1]. The orientational properties, and particularly the strength and the range of the anchoring forces, depend strongly on the chemical natures of the LC and of the surface, and may be completely different at different interfaces. Indeed, treating substrates with various coupling agents can produce a surface that orients the same liquid-crystal molecules normal to the substrate or in a planar arrangement parallel to the substrate [1]. This is important for the design of many LC devices. Surfaces can also induce structural ordering at the interfaces. Several groups have reported recently on surface-ordering effects in LC in the vicinity of the nematic-isotropic [2,5,6], smectic-nematic [7], and smectic-isotropic [8,9] phase transition. Of particular interest, in this respect, is the work of Ocko [8] who carried out x-ray-reflectivity studies at the LC-solid and at the LC-air interfaces; he found that the anchoring field strength at the latter interface is stronger.

This paper is concerned with thin films of the ferroelectric liquid crystal, ZLI-3654. This ferroelectric LC was chosen because it is often used in light-valve devices, the so-called surface-stabilized ferroelectric-liquid-crystal (SSFLC) cells [10–12]. There is, therefore, some information on its orientational wetting properties at the substrate-LC interface in SSFLC cells. An essential feature of these cells is the presence of an "alignment layer" in the form of rubbed polymer or SiO evaporated at an oblique angle which effectively induces uniaxial planar alignment in the LC [10]. This usually results in tilted smectic planes (chevron structure [11,13]) in the smectic-C^* phase and smectic planes perpendicular to the substrate in the smectic-A phase. There are other substrates which are less effective but nevertheless tend to induce planar alignment which becomes uniaxial planar ("homogeneous") by microgrooving the substrate [1]. Among such substrates are glass slides and indium-tin-oxide-glass. In contrast, experiments [1,14] on several types of LC's and computer simulations [5] have shown that the alignment of the LC molecules at the LC-air interface is normal to the substrate. The question arises: What are the structural properties of ultrathin films (thickness smaller than the penetration depth, ξ, of the anchoring forces) sandwiched between a solid substrate (such as rubbed polymer on glass) and air? Generally, the structure of such a film is influenced by the anchoring forces at both the substrate-LC and the LC-air interfaces, but it is unknown, at present, which dominates.

In addition to the question of competing orientations induced at the two interfaces, there are many other questions concerning the nature of the phases and the phase transition in ultrathin LC films. As was shown previously [16], anchoring forces at interfaces increase the phase-transition temperature. On the other hand, finite-size effects may play an important role [17] including (i) a smearing of the phase transition and (ii) shifting of the phase-transition temperature to lower values.

This paper reports on x-ray reflectivity of thin films of a ferroelectric chiral smectic-C^* (Sm-C^*) liquid-crystal mixture on various substrates but with the main emphasis on float glass. We found that spin casting of diluted solutions of the ferroelectric liquid-crystal mixture ZLI-3654, on all the substrates leads to stable, well-oriented thin films with smectic layers parallel to the substrate. We

show that this alignment is induced by the film-air interface. We demonstrate also that the specular x-ray reflectivity provides information on various structural properties of ultrathin films but particularly on the smectic layer spacing, L, and the film thickness, d. The fitting procedure to our model is very sensitive to any change of these parameters. Both L and d are strongly temperature dependent. This is attributed to the temperature dependence of the molecular tilt angle, α, which is the angle between the director of the LC molecules and the normal to the smectic layers. Thus, x-ray reflectivity allows determination of the tilt angle in ultrathin films. The tilt angles in thin films are compared with those measured in the bulk using the high-resolution x-ray technique [18].

II. MODEL

In this section, we briefly describe a simple model, developed by Entin, Goffer, and Davidov [16] which will be used for the evaluation of our data. We consider an ordered film on a float-glass substrate with smectic layers parallel to the substrate. The corresponding density profile in the direction normal to the substrate surface (which we chose as the z direction) is schematically presented in Fig. 1, where (1), (2), and (3) designate the glass substrate, the LC film and the air, respectively. We assume that the electron density in the LC film, $\rho_2+\delta\rho$, is periodically modulated and can therefore be described by a Fourier series,

$$\delta\rho(z)=\frac{1}{2}\rho_2\sum_{n=1}^{\infty} w_n \exp\left[i\left[\frac{2\pi nz}{L}+\varphi_n\right]\right]+\text{c.c.}\ , \tag{1}$$

where L is the thickness of one smectic layer and ρ_2 is the average density of the film. In a finite-size film the density modulation leads to quasi-Bragg peaks; the first harmonic is centered around $\theta_B\cong\lambda/2L$, where λ is the x-ray wavelength ($\lambda=1.54$ Å). The total specular reflectivity, R, is a result of interference between the coherent beams scattered by the interfaces and the density modulation

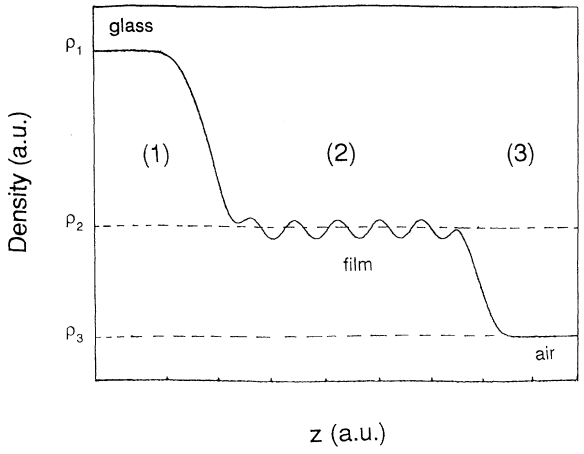

FIG. 1. Schematic representation of the density profile along the z axis (perpendicular to the film) of a system composed of the glass substrate (1), the LC film (2), and air (3); ρ_i ($i=1,2,3$) are the appropriate electronic densities related to the parameters δ_i.

$$R=[r+r_B]^2\ , \tag{2}$$

where r is the reflected complex amplitude (Kiessig oscillations [19]) from the interfaces and r_B is the reflected amplitude arising from the density modulation. For films sandwiched between two interfaces (Fig. 1), r is given by the well-known formula [20]

$$r=\frac{r_{23}+r_{12}\exp(2ik_2d)}{1+r_{12}r_{23}\exp(2ik_2d)}\ . \tag{3}$$

Here d is the thickness of the film, r_{12} and r_{23} are the Fresnel reflection coefficients from the interfaces 1-2 (substrate-film) and 2-3 (film-air), respectively, and k_2 represents the z component of the wave vector in the film. For a three-interface system, a formula analogous to Eq. (3) was given by Russel [20]. Assuming interfacial roughnesses that can be described in the density profile by error functions at the interfaces, the reflected complex amplitudes r_{ij} can be expressed as follows [20]:

$$r_{ij}=\frac{k_i-k_j}{k_i+k_j}\exp(-2k_ik_j\sigma_{ij}^2)\ , \tag{4}$$

where σ_{ij} is the width of the rough interface i, j, and k_j are the z components of the wave vector in the jth medium, given by

$$k_j=\frac{2\pi n_j}{\lambda}\sin\theta_j\ , \tag{5}$$

θ_j are the angles of incidence at the interface ($j,j-1$) (as determined by Snell's law), and n_j are the complex refractive indices ($n_j=1-\delta_j-i\beta_j$, where $\delta_j=\lambda^2\rho_jr_e/2\pi$) [20]. Since the Bragg scattering angle, θ_B, is significantly larger than the critical angle for total reflection, θ_C [20], the reflected amplitude r_B, can be calculated in the framework of the first Born approximation [20,21] by a Fourier transform of the electron-density derivative, $d\rho/dz$, across the film. Considering only the first harmonic in Eq. (1), r_B can be calculated as

$$r_B\cong\frac{\lambda^2r_e\rho_2w}{4L\theta^2}\frac{\exp(-i\varphi)\left\{\exp\left[i\left[2k_2-\frac{2\pi}{L}\right]d\right]-1\right\}}{\frac{2\pi}{L}-2k_2}\ . \tag{6}$$

Here $r_e=e^2/mc^2$ is the classical electron radius, φ and w denote the phase and the amplitude appropriate to the first harmonic [in Eq. (1)], and θ is half of the scattering angle which is related to θ_j by Snell's law.

It is noteworthy that because of the cross term of Eq. (2), the phase φ enters explicitly into the final expression and has a strong influence on the shape of the reflectivity profile. It is also worthwhile to mention that usually the Bragg-like reflection in thin films, r_B^2, is rather small. However, the experimentally observed Bragg-like reflection is significantly enhanced by the cross term in Eq. (2). It is this enhancement which allows a study of smectic ordering in ultrathin films consisting of only a few smectic layers.

Finally, several authors have demonstrated that the amplitudes of the density modulation and the periodicity L may vary across the film [22]. Particularly the layer spacing at the interfaces may differ from the interior layer in films of liquid crystals [7–9]. Our model can be easily generalized to include such variation. However, this involves a significant increase in the number of the fitting parameters (which is already large even for a simple sinusoidal density modulation).

III. DATA EVALUATION, EXPERIMENT

Combining Eqs. (2), (3), and (6) leads to an expression describing the reflected intensity in the angular range: $\theta_C \leq 2\theta \leq 4°$ (above $2\theta \cong 3.5°$ the diffuse scattering becomes significant and the fit should be regarded with caution; below 0.5° the x-ray-reflected intensity is very high leading to nonlinear response of our detector).

The fitting procedure employs the Nedler-Meade simplex algorithm [23] and involves ten free parameters, which are not completely uncorrelated, namely, the film thickness, d, the layer spacing, L, the substrate-film roughness parameter, σ_{12}, the film-air roughness parameter, σ_{23}, the density modulation amplitude, w, the phase, φ, and the parameters δ_1, δ_2, β_1, and β_2 related to the complex refraction indices. For the glass substrate δ_1 and β_1 were calculated [20] independently, using standard tables of atomic form factors ($\delta_1 = 7.5 \times 10^{-6}$ and $\beta_1 = 9.7 \times 10^{-8}$). For the LC film, β_2 is negligible. The remaining seven free parameters, namely, δ_2, σ_{12}, σ_{23}, d, L, ϕ, and w, turned out to be hardly correlated in the fitting procedure. This fitting is very sensitive to any change in the values of d and L and less sensitive to the value of δ_2.

The ferroelectric LC mixture ZLI-3654 was provided by Merck. This liquid-crystal mixture has rather low-viscosity, room-temperature smectic-C^* phase and high-quality (quality determined by the x-ray reflectivity) thin films can be prepared using the spin-coating technique. The bulk transition temperatures are shown in the following diagram [24]:

$$\text{crystalline} \underset{243\ \text{K}}{\longrightarrow} \text{Sm-}C^* \underset{335\ \text{K}}{\longrightarrow} \text{Sm-}A \underset{349\ \text{K}}{\longrightarrow} \text{cholesteric} \underset{359\ \text{K}}{\longrightarrow} \text{isotropic} .$$

Films were prepared by dissolving the LC in toluene and casting the solution onto a substrate using a Headway PM 101D photoresist coater. Film thicknesses (100–800 Å) were controlled by varying the concentration (0.5 to 2.6 wt. %) and the speed of the coater (~4000 rpm). The films so prepared exhibit a remarkable stability (over more than several months in air) and uniformity. Although during measurements the film substrate was held in an upright position, we have not seen any evidence for a flow of the LC, even in the isotropic phase. We have used the following different substrates: (a) very smooth (float) glass; (b) float glass coated with indium tin oxide (ITO); (c) Si wafers; (d) float glass coated with polymer (mainly nylon); (e) rubbed nylon on float glass. Although we demonstrate some x-ray-reflectivity data of films on such substrates (Fig. 2), the main emphasis in this work is on float-glass substrates (Figs. 3 and 4). Float-glass substrates with an area of 4×4 cm^2 with surface roughnesses of 3 Å to 4 Å were used. Prior to the casting procedure the glass substrates were cleaned in a H_2SO_4-H_2O_2 mixture. Details of the preparation of films on substrates other than float glass will be given elsewhere.

The reflectivity setup is based on high-resolution x-ray spectrometer described elsewhere [25]. The actual measurements consists of θ–2θ scans (scanning along k_z) using a well-collimated Cu $K\alpha$ ($\lambda = 1.54$ Å) beam from a narrow-line source of a 12-kW Rigaku rotating anode. The half width at half intensity of the zero beam was ~0.02° (using a Ge monochromator with narrow slits but removing the analyzer). The background signal never exceeds several counts per second. A deconvolution technique assuming a one-dimensional triangular resolution function was employed whenever necessary. However, in most of the data analysis presented here deconvolution was not necessary.

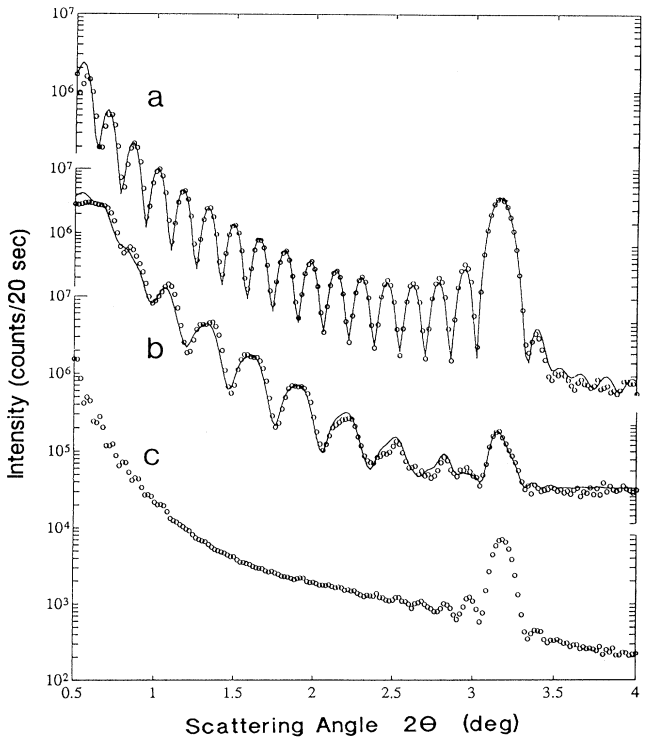

FIG. 2. Reflectivity profiles of thin ZLI-3654 films on various substrates: (a) silicon, (b) glass covered with ITO, (c) glass covered with rubbed nylon. Note the clear quasi-Bragg peak, at approximately 3.2°, in all cases. The open circles represent experimental data. The solid lines in (a) and (b) represent a fit to our model. In (b) the fitting procedure is more complicated due to the presence of a three-interface system and will be discussed elsewhere. In (c), the nylon surface is too rough to allow any analysis. The x-ray wavelength is $\lambda = 1.54$ Å.

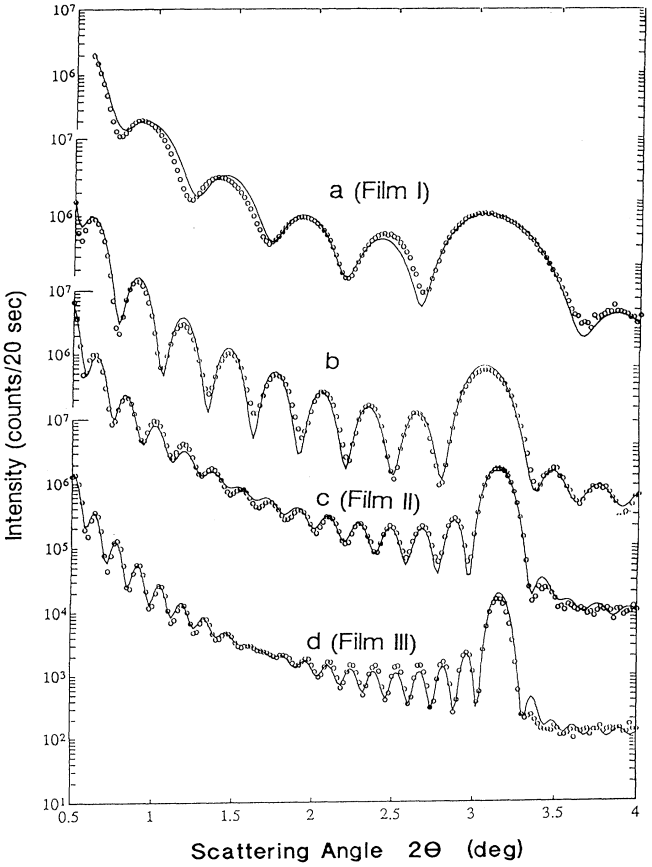

FIG. 3. X-ray-reflectivity profiles of ZLI-3654 as cast films having different thicknesses (a) 180 Å (film I), (b) 306 Å, (c) 451 Å (film II), (d) 614 Å (film III). The open circles represent experimental data. The solid lines represent the best fits of the model. The corresponding parameters are listed in Table I, for films I, II, III. The x-ray wavelength is $\lambda = 1.54$ Å.

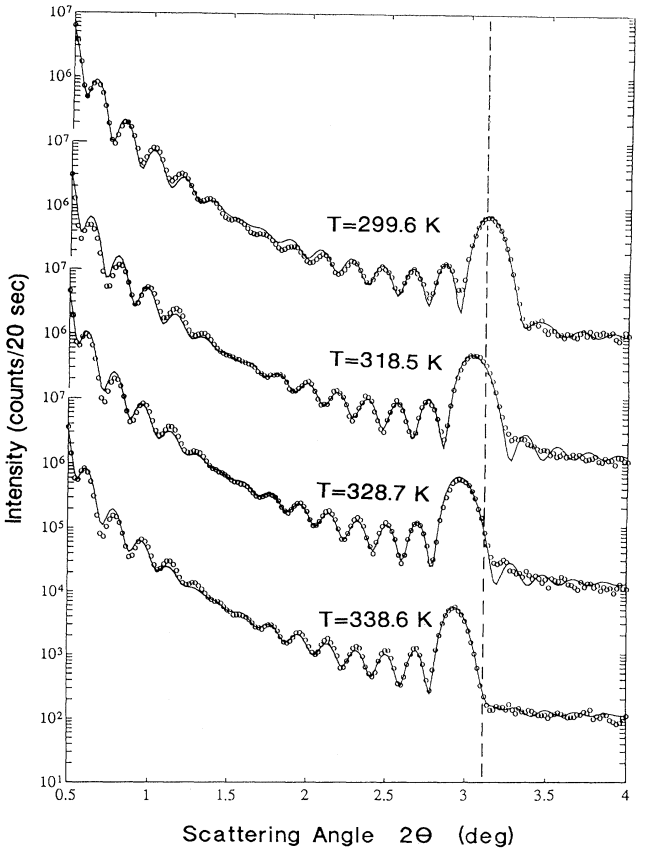

FIG. 4. X-ray-reflectivity profiles of film II at various temperatures. The open circles represent experimental data. The solid lines represent the best fits to our model. The corresponding fitting parameters are listed in Table II. The vertical dashed line is a guide to the eye to emphasize the shift of the quasi-Bragg peak with temperature. The x-ray wavelength is $\lambda = 1.54$ Å.

The films on the substrate were stood upright under atmospheric pressure inside an oven [25]. This oven has a long-term temperature stability better than 0.1 K. Temperature homogeneity better than 0.2 K over the entire film was achieved by special copper shielding.

IV. RESULTS

As-cast films of ZLI-3654 on various substrates were studied at room temperature. Figures 2 and 3 show some of the x-ray-reflectivity profiles of these films. A main feature in all the reflectivity spectra (Figs. 2 and 3) is the appearance of a quasi-Bragg peak at $2\theta \cong 3.2°$. This feature is independent of the particular substrate and strongly suggests the formation of smectic layers parallel to the substrate with a layer spacing of ~ 28 Å. We emphasize that without ordering and coherence it is practically impossible to observe Bragg-like peaks in such thin films. We observe ordered films with smectic layers parallel to the substrate even on substrates which usually induce planar alignment in SSFLC cells (such as a rubbed nylon film on glass). Among the many films measured (Figs. 2 and 3), we concentrate here on three films of ZLI-3654 on float glass designated as film I ($d \sim 180$ Å), film II ($d \sim 451$ Å), and film III ($d \sim 614$ Å). The film thickness at room temperature roughly corresponds to 6(I), 16(II), and 22(III) smectic layers, respectively.

Figure 3 shows the x-ray specular reflectivity spectra of the as-cast films (I, II, and III). The solid lines in the same figure represent the best fit to the model. The fit matches most of the data points within their error range and indicates that the smectic layering parallel to the substrate can be described by a one-dimensional sinusoidal density modulation across the films. In view of the very good fits, we have not made many attempts to fit the data to a more complicated density modulation. We note that the layer spacing, L, may depend slightly on z but, apparently, the fitting procedure is not very sensitive to a small variation of $L(z)$. Thus, the value of L extracted from the fitting procedure should be considered as an "average" value for each film. The parameters extracted from the fitting procedure are given in Table I for the as casted films I, II, and III on glass. The most important parameters for our discussion are the film thickness, d,

TABLE I. Parameters describing the reflected intensity of different ZLI-3654 films on float glass. These parameters were extracted from the fitting procedure (solid lines in Fig. 3). δ_2 is related to the electronic density of the film; σ_{12}, the glass-film roughness parameter; σ_{23}, the film-air roughness parameter; d, the film thickness; L, the layer thickness; φ, the phase of the density modulation with respect to the LC-air interface; and w is proportional to the amplitude of the electronic density modulation. The errors in Tables I and II are associated with the fitting to the model and represent a range in which the fits are very reasonable.

	$\delta_2\times10^6$	σ_{12} (Å)	σ_{23} (Å)	d (Å)	L (Å)	φ (rad)	w	d/L
Film I	2.2±0.4	7.5±1.0	7.6±1.1	180±2	28.1±0.1	−1.7±0.1	0.34±0.02	6.4±0.1
Film II	3.4±0.4	5.6±1.0	17.6±2.5	451±3	28.1±0.1	0.0±0.1	0.11±0.1	16.0±0.2
Film III	3.3±0.4	2.5±0.5	13.1±2.2	614±3	28.0±0.1	0.1±0.1	0.22±0.01	22.0±0.2

and the layer thickness, L. The ratio d/L provides the number of layers, n. Clearly, d/L is not always an integer, suggesting that d and L are not always commensurate (Table I). The film thickness is determined by the spin-coating procedure. The number of layers must be adjusted accordingly. It is possible that domains with different number of layers are formed in the lateral direction. This can explain the noninteger values we got for n and probably also the roughness at the film-air interface (about one-half of a layer spacing for thick films). The roughness parameters σ_{12} and σ_{23} change significantly from one film to another (Table I) ranging from 3 to 8 Å for the glass-LC interface and from 3 to 30 Å for the LC-air interface. Roughness turned out to be strongly preparation dependent but, generally speaking, the roughness increases with the film thickness (Fig. 3).

X-ray reflectivity versus temperature studies were carried out in the temperature range 300 to 342 K with the aim to explore the Sm-A–Sm-C^* phase transition. It was essential to anneal the film at ~342 K (above the phase transition) for several hours to obtain reproducible results. After such heat treatment there are some changes in the reflectivity profiles as compared to the as cast film. The reflectivity spectra are completely reversible after the first temperature cycle. Measurements were carried out in steps of ~1.5 K. The temperature was changed very slowly (~0.1 K/min) and at each temperature the sample was annealed for an hour to ensure thermal equilibrium.

Figure 4 shows some of the reflectivity profiles of film II at various temperatures. The solid lines represent the best fits with the parameters given in Table II. Note (Fig. 4) the change in the position of the quasi-Bragg peak with increasing temperature, i.e., a shift from $2\theta\cong3.14°$ ($T=299$ K) to $2\theta\cong2.94°$ ($T=338$ K) corresponding to a change in the layer spacing from $L\cong28.1$ Å to $L\cong29.9$ Å. Also the number of Kiessig oscillations in the evaluated range increases, which means that the film thickness increases. Figure 5 shows the layer spacing, L, of the films I, II, and III as a function of temperature. Clearly, there is a monotonic change of L below ~330 K. Above this temperature L seems to fluctuate around a constant value. We identify this behavior as arising from a phase transition from the smectic-A phase to the smectic-C^* phase with a phase-transition temperature, T_c, near 330 K (but see below). Note also the remarkable increase of the smectic layer spacing in ultrathin films (~200 Å) (see film I in Fig. 5). Although this behavior is consistent with previous observations by others [26,27], it is not completely understood at present. Plotting the thicknesses, d, of the different films against their layer spacings, L, (Fig. 6) we observe a linear relation. The average slopes $\langle d/L\rangle$ ($\langle d/L\rangle\cong n$) are given in Table III. The roughness parameters σ_{12} and σ_{23} are almost independent of temperature (Table II). We emphasize that the errors in Tables I and II are associated with the fitting to the model and represent a range in which the fits are very reasonable.

V. DISCUSSION

We have shown that, by the spin-casting technique, it is possible to produce large-area "single-domain" samples of liquid-crystal films with smectic layers parallel to the substrate. The alignment is independent of the particular substrate and was observed even on rubbed nylon surfaces which are known to induce planar alignment in SSFLC cells. We conclude, therefore, that it is the anchoring force at the film-air interface which is responsible for the ordering in these smectic LC films. In contrast, previous studies have shown that the side-chain polymeric liquid crystal, PMA, order only on float-glass substrate

TABLE II. Parameters describing the reflected intensities of film II at different temperatures, corresponding to the solid lines in Fig. 4. The various parameters are defined in the text or in the caption of Table I.

Temp. (K)	$\delta_2\times10^6$	σ_{12} (Å)	σ_{23} (Å)	d (Å)	L (Å)	φ (rad)	w	d/L
299.6±0.2	3.4±0.4	5.6±1.0	17.6±2.5	451±3	28.1±0.1	0.0±0.1	0.11±0.01	16.0±0.2
318.5±0.2	3.4±0.4	4.8±1.0	18.4±2.7	469±3	29.0±0.1	0.0±0.1	0.11±0.01	16.2±0.2
328.7±0.2	3.3±0.4	6.0±1.0	19.8±2.9	480±3	29.7±0.1	0.0±0.1	0.10±0.01	16.2±0.2
338.6±0.2	3.3±0.4	5.7±1.0	20.8±3.0	480±3	29.9±0.1	0.0±0.1	0.09±0.01	16.0±0.2

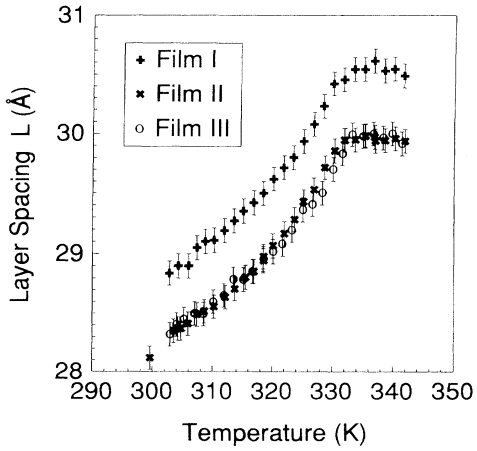

FIG. 5. Smectic layer spacing, L, of different ZLI-3654 films as a function of temperature. For comparison, the smectic layer spacing of the bulk is 29.7 Å in the smectic-A phase.

and not on Si, suggesting that the alignment here is induced by the glass-substrate–polymer interface [16]. The possibility that the alignment is induced by the spin-coating procedure is rejected because the shear gradients normal to the substrate during the spinning are expected to align the molecules parallel to the surface, in contrast to our observations.

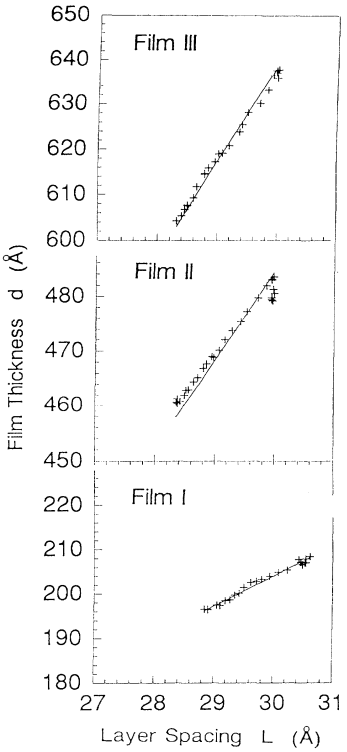

FIG. 6. Thickness, d, of different ZLI-3654 films as a function of smectic layer spacing, L. The solid lines represent linear fits. The slopes give the average ratio $\langle d/L \rangle$ quoted in Table III.

TABLE III. Parameters excited from the fit of Eq. (7) to the temperature dependence of the tilt angle $\alpha(T)$ (Fig. 7). T_c is the Sm-C^*–Sm-A phase-transition temperature and γ is a critical exponent. Note the similarities of T_c and γ to the bulk value.

	$\langle d/L \rangle$	α_0 (deg)	T_c (K)	γ
Film I	6.80±0.2	41±3	330.4±1.4	0.30±0.03
Film II	16.19±0.2	45±2	330.7±1.4	0.34±0.02
Film III	21.29±0.2	48±4	331.8±1.8	0.29±0.04
Bulk [18]		40±2	332.2±0.1	0.31±0.01

A simple model which assumes sinusoidal density modulation across the ZLI-3654 film can fit the reflectivity profile well (Figs. 3 and 4). This indicates that the assumptions concerning the coherence of the reflected beams in the model is correct. It also suggests that the alignment induced by the film-air interface is complete (complete wetting) and that the coherence length, ξ, associated with the anchoring force exceeds the film thickness, $\xi > 800$ Å. We note (Tables I and II) that the phase φ is almost zero in most of our reflectivity profiles. The phase measures the shift of the density modulation with respect to the film-air interface and the observation of $\varphi = 0$ suggests that the maximum of the sinusoidal density is at this interface. At the present time, the nature of the anisotropic chemical interactions which are responsible for the anchoring force is not clear. However, we feel that the LC-air surface tension and the relatively low rotational viscosity may play an important role.

The results in Fig. 5 indicate that the layer spacing, L, is almost constant above $T_c \cong 330 \pm 2$ K but monotonically decreases below this temperature. Also the film thickness, d, monotonically decreases as shown by the linear relation between d and L (Fig. 6). We attribute these changes to the change of the tilt angle, α, in the smectic-C^* phase. Considering the LC molecules as rigid rods, the tilt angle is related to the layer thickness as $\alpha(T) = \arccos[L(T)/L_0]$, where L_0 is the layer thickness in the smectic-A phase. L_0 was estimated by averaging the values of L above the phase-transition temperature, giving $L_0 = 30$ Å for films II and III and $L_0 = 30.5$ Å for film I (Fig. 5); $L(T)$ is the layer thickness at a given temperature, T. Figure 7 exhibits a plot of $\alpha(T)$ for the three films. The results can be described well by the formula [18,28]

$$\alpha(T) = \alpha_0 \left[1 - \frac{T}{T_c} \right]^{\gamma}, \tag{7}$$

where T_c is the smectic-A–smectic-C^* phase transition temperature and γ is a critical exponent. The solid lines in Fig. 7 represent our best fits using the parameters α_0, T_c, and γ in Table III. The same figure and table provide information on the tilt, $\alpha(T)$, as measured on a bulk material of ZLI-3654 using a high-resolution x-ray technique [18]. In all cases, T_c is approximately the same as in the bulk. The average critical exponent in the films is

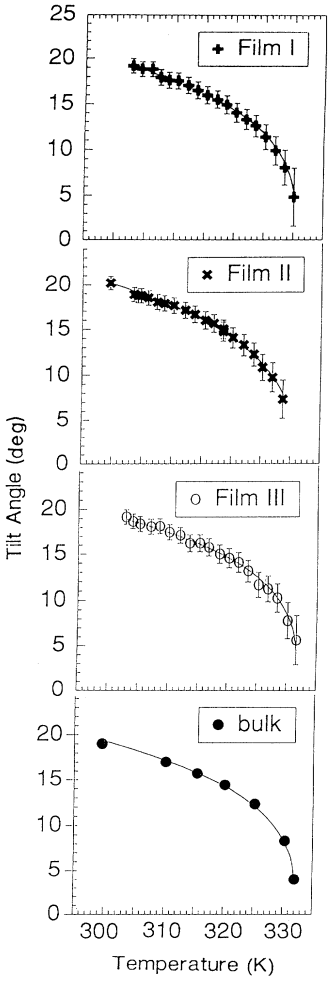

FIG. 7. Tilt angles versus temperature, as extracted from Fig. 5, for the different ZLI-3654 films (films I, II, and III). For comparison we show the tilt angle extracted from bulk material measurements using high-resolution x-ray technique [18]. The solid lines are the best fits to the power law, Eq. (7). The corresponding parameters are listed in Table III.

$\gamma \cong 0.31 \pm 0.04$. This exponent is the same as the bulk value and in agreement with the predicted analogy with the Bose condensation in superfluid helium [28]. The observation of similar tilt angles in thin films and in the bulk further supports our assumption concerning the density modulation.

The results in Table III suggest that the nature of the smectic-C^* phase and the Sm-A–Sm-C^* phase-transition temperature are not affected by the film thickness. This implies that the LC interactions are very strong compared to interactions with the substrate and the smectic-C^* properties are maintained even in films of only a few smectic layers. This is very surprising in view of theoretical predictions [17]. Apparently, finite-size effects are not important. In contrast to the results presented here, previous x-ray-reflectivity studies of a thin LC film on a substrate indicate some increase in the Sm-A–N phase-transition temperature in a PMA polymeric liquid crystal [16] and a significant decrease of the Sm-A–Sm-C^* phase-transition temperature in films of the ferroelectric mixture FELIX 008 [27] (provided by Hoechst AG, Germany).

Finally, the changes in the tilt angle and the layer thickness across the Sm-A–Sm-C^* phase transition lead to change in the film thickness, d, of almost $(7\pm2)\%$ (Fig. 6). This remarkable change is associated with a large volume change across the phase transition and probably large changes in the electronic density (although this is not clear, due to the large error in the density, see Table II). We note that the change in the density across the Sm-A–Sm-C^* phase transition is significantly smaller [29] in bulk of LC's. It would be of interest to verify if such large changes in the film thickness and density are associated with changes in the optical properties of the film. The thin films presented here may have applications as planar optical wave guides provided that the films exhibit high structural and optical quality in the lateral direction (x-y plane).

Note added in proof. After this paper was submitted for publication, we studied the quality of films of ZLI-3654 prepared by the spin-coating technique on rough glass surfaces. We have used the metallurgical optical microscope and atomic force microscope at the Curie Institute, Paris. These observations indicate the presence of domains in the x-y plane of the films and the presence of liquid-crystal droplets on the films. At the present time, we cannot use the existing setup to study our own films, which are prepared on very smooth surfaces. The high quality of our x-ray-reflectivity data suggests, however, that the density of LC droplets on our films is small, if any. The microscopic studies do not change any of the conclusions of this paper. We thank G. Cohen and D. Chatenay for their efforts.

ACKNOWLEDGMENTS

This work was supported by research grants from the European Community, the Israeli Ministry of Science and Technology, and the German-Israeli Foundation (GIF). We gratefully acknowledge support from Minerva that made it possible for one of us (E.O.) to stay in Jerusalem. We wish to thank Dr. I. Entin for providing us his program for the nonlinear least-square fits and for many helpful discussions. G. Cohen prepared the first sample and therefore initiated our work. Professor Pincus, Dr. Golosovsky, and Dr. Golub are acknowledged for interesting discussions.

[1] F. J. Kahn, Phys. Today **35**(5), 66 (1982); P. Sheng, Phys. Rev. A **26**, 1610 (1982).
[2] W. Chen, L. J. Martinez-Miranda, H. Hsiung, and Y. R. Shen, Phys. Rev. Lett. **62**, 1860 (1989).
[3] D. W. Allender, G. L. Henderson, and D. L. Johnson, Phys. Rev. A **24**, 1086 (1981).
[4] M. M. Telo da Gama, Mol. Phys. **52**, 585 (1984).
[5] S. Immerschitt, T. Koch, W. Stille, and G. Strobl, J. Chem. Phys. **96**, 6249 (1991).
[6] K. Miyano, Phys. Rev. Lett. **43**, 51 (1979).
[7] P. S. Pershan, A. Braslau, A. H. Weiss, and J. Als-Nielsen, Phys. Rev. A **35**, 4800 (1987); B. M. Ocko, A. Braslau, P.

S. Pershan, J. Als-Nielsen, and M. Deutsch, Phys. Rev. Lett. **57**, 94 (1986).
[8] B. M. Ocko, Phys. Rev. Lett. **64**, 2160 (1990).
[9] D. J. Tweet, R. Holyst, B. D. Swanson, H. Stragier, and L. B. Sorenson, Phys. Rev. Lett. **65**, 2157 (1990); R. Holyst, D. J. Tweet, and L. B. Sorenson, *ibid.* **65**, 2153 (1990).
[10] G. Cohen, D. Davidov, L. Lifshitz, E. Nachaliel, and C. Escher, Ferroelectrics **132**, 87 (1992).
[11] N. A. Clark and T. P. Rieker, Phys. Rev. A **37**, 1053 (1988).
[12] N. A. Clark and S. T. Lagerwall, Appl. Phys. Lett. **36**, 899 (1980).
[13] T. P. Rieker, N. A. Clark, G. S. Smith, D. S. Parmer, E. B. Sirota, and C. R. Safinya, Phys. Rev. Lett. **59**, 2568 (1987).
[14] R. A. M. Hikmet, Adv. Mater. **4**, 697 (1992).
[15] L. Lifshitz (private communication).
[16] I. Entin, R. Goffer, and D. Davidov, Phys. Rev. B **47**, 8265 (1993).
[17] K. Binder, Ferroelectrics **73**, 43 (1987).
[18] R. Halfon, E. N. Keller, E. Nachaliel, D. Davidov, and C. Escher, Ferroelectrics **114**, 345 (1991).
[19] H. Kiessig, Ann. Phys. (Leipzig) **10**, 769 (1931).
[20] T. P. Russel, Mater. Sci. Rep. **5**, 171 (1990).
[21] M. Born and E. Wolf, *Principles of Optics* (Pergamon, Oxford, 1975).
[22] A. Menele, T. P. Russel, S. H. Aanastasiadis, S. K. Satija, and C. F. Majkrzak, Phys. Rev. Lett. **68**, 67 (1992).
[23] J. A. Nedler and R. Meade, Comput. J. **7**, 308 (1965).
[24] E. Merck, preliminary data sheet, Merck AG, Darmstadt, Germany, 1986. Note that the Sm-A–Sm-C^* phase-transition temperature as measured by high-resolution x-ray technique (see Halfon *et al.*, Ref. [18]) is slightly lower ($T_c = 332.2$ K).
[25] E. Nachaliel, E. N. Keller, D. Davidov, and C. Boeffel, Phys. Rev. A **43**, 2897 (1991); I. Belaish, Ph.D. thesis, Hebrew University, 1991.
[26] H. Menzinger, M. Stamm, and C. Boeffel, J. Chem. Phys. **96**, 3183 (1992).
[27] M. Tarabia *et al.* (unpublished).
[28] P. G. de Gennes, C. R. Acad. Sci. Ser. B **274**, 785 (1972).
[29] R. Kiefer and G. Baur, Liq. Cryst. **7**, 815 (1990).